

Transcription factor MAFA regulates muscle growth via calcium ion channels and receptor tyrosine kinase activation

Cuiyu Lai ^{a,b,1}, Yang Chen ^{a,b,1}, Xuewen Han ^{a,b}, Yu Fu ^{a,b}, Jinlin Chen ^{a,b}, Dandan Tan ^{a,b}, Xuesong Shan ^{a,b,*}, Huaizhi Jiang ^{a,b,*}

^a College of Animal Science and Technology, Jilin Agricultural University, Changchun 130118, China

^b Key Laboratory of Animal Production and Product Quality and Safety, Ministry of Education, Changchun 130118, China



ARTICLE INFO

Keywords:

MAFA
Skeletal muscle
Calcium influx
INSR
EGFR
FOXO3

ABSTRACT

MAFA, a member of the large Maf transcription factor family, is known primarily for its role in regulating insulin gene expression. However, its function in non-pancreatic tissues remains largely unexplored. This study aims to investigate the role of MAFA in skeletal muscle and to elucidate the underlying molecular mechanisms. Quantitative PCR analysis showed that MAFA is highly expressed in sheep skeletal muscle, and its expression level is positively correlated with muscle mass. By integrating ChIP-Seq and RNA-Seq data from longissimus dorsi muscle, we identified that MAFA preferentially binds and regulates genes enriched in calcium signaling and receptor tyrosine kinase (RTK)-related pathways. Functional studies were conducted in primary sheep myoblasts using MAFA overexpression and siRNA-mediated knockdown. These gain- and loss-of-function assays demonstrated that MAFA promotes myoblast proliferation and inhibits differentiation. Mechanistically, MAFA upregulates STIM1 and PPP3CA, promoting intracellular Ca^{2+} influx. In parallel, MAFA transcriptionally activates INSR and EGFR, thereby enhancing PI3K/Akt signaling and inducing phosphorylation-dependent nuclear exclusion of FOXO3, a key catabolic transcription factor. These findings suggest that MAFA may play an important regulatory role in skeletal muscle development through calcium- and RTK-mediated signaling pathways, offering new insights into muscle biology and potential targets for improving livestock production and muscle-related disorders.

1. Introduction

MAFA (MAF BZIP Transcription Factor A) belongs to the large MAF family of basic leucine zipper (bZIP) transcription factors [1–4]. It is best known for its pivotal role in pancreatic β -cells, where it binds to the *insulin* (*INS*) promoter and drives insulin transcription and secretion [5,6]. MAFA contributes critically to glucose homeostasis and has been proposed as a therapeutic target for type 2 diabetes [7,8]. Notably, ectopic overexpression of MAFA can reprogram pancreatic α -cells into insulin-producing β -like cells [9]. While extensive studies have explored the role of MAFA in regulating insulin gene transcription in pancreatic β -cells, its functions in other tissues remain largely unexplored. Unlike other members of the large Maf transcription factor family—such as MAFB and c-MAF—which have been implicated in diverse developmental processes, research specifically focusing on MAFA in non-endocrine systems is still limited. Notably, recent evidence has

revealed that MAFA is also expressed in skeletal muscle, suggesting a broader functional spectrum than previously appreciated. However, to date, only a few studies have directly investigated the role of MAFA in muscle biology. For example, Sadaki et al. demonstrated that members of the large Maf family regulate type IIb myofiber identity [10], and Ring et al. and Huang et al. reported related transcriptional roles for Maf genes in lens and cartilage tissues, respectively [11,12]. These findings raise the possibility that MAFA may participate in the regulation of skeletal muscle development and fiber-type specification, warranting further investigation.

Skeletal muscle is the largest organ in mammals, accounting for 30–50 % of total body mass [13,14]. It plays essential roles in locomotion, posture, and systemic metabolism. Muscle tissue is a major site for insulin-stimulated glucose uptake through GLUT4 translocation [15,16], and muscle mass is a critical determinant of whole-body insulin sensitivity, especially under conditions of obesity, aging, or metabolic

* Corresponding authors at: College of Animal Science and Technology, Jilin Agricultural University, Changchun 130118, China.

E-mail addresses: shansong@jlu.edu.cn (X. Shan), jianghz6806@126.com (H. Jiang).

¹ Cuiyu Lai and Yang Chen contributed equally to this work.

stress [17–19]. Conversely, insulin signaling also contributes to muscle development and protein synthesis, emphasizing the bidirectional relationship between metabolic regulation and muscle biology [20,21].

The formation of skeletal muscle fibers, or myogenesis, is a tightly regulated, multi-stage process [22–24]. During embryogenesis, mesodermal progenitors differentiate into mononucleated myoblasts, which subsequently fuse to form primary and later secondary multinucleated myotubes. Postnatally, muscle growth proceeds predominantly through hypertrophy, fiber remodeling, and fiber type switching, rather than an increase in fiber number. These processes are orchestrated by myogenic regulatory factors (MRFs), such as Myf5, MyoD, Myogenin (MyoG), and MRF4/MEF2C, which coordinate the balance between myoblast proliferation and differentiation [25,26]. At the same time, multi-level interactions between the genome, epigenome, and environment influence overall growth and development [27,28]. Gene expression in eukaryotes is also temporally and tissue-specifically regulated, with only a subset of genes actively transcribed at any given stage [29], adding further complexity to transcriptional regulation. Consequently, understanding the regulation of skeletal muscle development through integrative multi-omics approaches is of considerable value for dissecting muscle biology.

Given MAFA's central role in insulin transcription and its expression in skeletal muscle, we hypothesized that MAFA may serve additional functions in regulating muscle growth. However, its role in skeletal muscle biology, particularly in large-animal models relevant to both agricultural and biomedical contexts, remains poorly understood. This represents a critical gap in our current knowledge: while MAFA has been extensively studied in the context of endocrine pancreas, its regulatory targets and molecular functions in skeletal muscle tissue have not been systematically investigated.

To address this gap, we conducted a comprehensive investigation of MAFA's role in skeletal muscle in a large-animal model (sheep). Sheep provide an ideal system to explore these functions due to their physiological similarities to humans in musculoskeletal traits and their importance in meat production. Not only are sheep more comparable to humans than rodents in terms of body size and physiology, but they also offer practical relevance for agricultural applications. In this study, we integrated chromatin immunoprecipitation sequencing (ChIP-seq), transcriptome profiling (RNA-seq), and muscle phenotype data to analyze the regulatory role and mechanisms of MAFA in skeletal muscle growth. To our knowledge, this is the first study to systematically map MAFA's genome-wide occupancy and transcriptional network in skeletal muscle of a livestock species. Integrative analysis revealed a set of MAFA-regulated candidate genes associated with muscle growth and development, which were functionally validated via MAFA overexpression and knockdown experiments.

Notably, MAFA target genes were significantly enriched in two major pathways: calcium signaling, which regulates myogenic differentiation via intracellular Ca^{2+} flux, and receptor tyrosine kinase (RTK)-mediated PI3K-Akt signaling, a canonical axis for promoting cellular growth, survival, and protein synthesis. This study offers multiple advances over previous work: it provides the first integrative ChIP-seq and transcriptomic map of MAFA activity in skeletal muscle, expands MAFA's known role beyond pancreatic β -cells, and utilizes a large-animal model with direct relevance to meat production and translational muscle biology. Together, our findings illuminate a novel transcriptional network in muscle and position MAFA as a molecular link between endocrine and musculoskeletal systems, with potential applications in livestock genetic improvement and metabolic disease intervention.

2. Materials and methods

2.1. Animals and sample collection

A total of 33 healthy female lambs, aged six months and with comparable body weights, were randomly selected from a crossbred

population of *Australian White × Small Tail Han* sheep. Animals were humanely euthanized via jugular vein exsanguination, following which body weight was recorded. The *longissimus dorsi* muscle was immediately dissected and weighed. *Longissimus dorsi* samples were collected from all animals, and additional tissues—including pancreas, testis, heart muscle, ovary, and subcutaneous adipose tissue—were collected from three randomly selected lambs for ChIP-seq or quantitative PCR analysis.

Tissue intended for transcriptome sequencing and quantitative PCR was rapidly snap-frozen in liquid nitrogen for 1 min and stored at -80°C . For ChIP-seq analysis, approximately 100 mg of fresh *longissimus dorsi* muscle or pancreatic tissue was sectioned into slices $<1\text{ mm}$ thick on ice and immediately crosslinked in PBS containing 1% formaldehyde (Sigma-Aldrich, cat. no. F8775) for 5–15 min on ice. Crosslinking was quenched by adding 1/20 volume of 2.5 M glycine (final concentration 125 mM), followed by gentle rocking for 5 min on ice. Samples were then washed three times with 1× PBS, centrifuged at $1000 \times g$ for 5 min at 4°C , and the supernatant was discarded. The resulting pellet was snap-frozen in liquid nitrogen for 1 min and stored at -80°C until further processing.

2.2. ChIP sequencing

The *longissimus dorsi* and pancreatic tissues ($n = 3$ per tissue) were cross-linked with formaldehyde and lysed to obtain whole-cell lysates. The chromatin was then sheared by sonication to yield DNA fragments of approximately 100–500 bp. Immunoprecipitation was performed using a MAFA-specific antibody (Cell Signaling Technology, #79737). The complexes were eluted and reverse cross-linked to recover the DNA.

The ChIP DNA was used to construct sequencing libraries with the NEBNext® Ultra™ DNA Library Prep Kit for Illumina (NEB, USA, #E7645L). End repair was performed by adding End Repair Reaction Buffer (10×) and End Prep Enzyme Mix, with incubation at 20°C for 30 min and 65°C for 30 min. Adapters were ligated using NEBNext Adaptor and Blunt/TA Ligase Master Mix at 20°C for 15 min, followed by treatment with USER Enzyme at 37°C for 15 min to remove uracil residues from the adapters. The products were purified using 1× AMPure XP beads. Library amplification was performed using 8–10 cycles of PCR with Universal PCR Primer and Index (X) Primer under the following conditions: 98°C for 10 s (initial denaturation), 98°C for 10 s (denaturation), 65°C for 30 s (annealing), and 72°C for 30 s (extension). After PCR, libraries were size-selected and purified with AMPure XP beads. Paired-end 150 bp (PE150) sequencing was performed on the Illumina NovaSeq™ 6000 platform.

Raw sequencing reads from IP and Input samples were processed using fastp (version 0.20.1) [30] for quality control, including adapter trimming, removal of duplicate and low-quality reads, and generation of clean data. Clean reads were aligned to the sheep reference genome (*Ovis_aries_rambouillet.ARS-UI_Ramb_v2.0*) using Bowtie2 (version 2.4.2) [31]. Duplicate reads were removed, and MACS2 (version 2.2.7.1) [32] was used to perform peak calling. Peaks were visualized using the Integrative Genomics Viewer (IGV) [33]. ChIPseeker [34], an R package, was used for peak annotation. Motif analysis was conducted using HOMER (v4.11.1). Differential peak analysis was carried out using DiffBind [35].

2.3. RNA sequencing

Total RNA was extracted from *longissimus dorsi* muscle samples ($n = 30 + 3$) and pancreatic tissues ($n = 3$). RNA concentration and purity were assessed using a NanoDrop 2000 spectrophotometer (Thermo Fisher Scientific), and RNA integrity was evaluated by agarose gel electrophoresis and Agilent 2100 Bioanalyzer (Agilent Technologies), with RNA integrity number (RIN) scores recorded. First-strand cDNA was synthesized by reverse transcription, followed by second-strand synthesis and adaptor ligation. Libraries were sequenced on the

Illumina NovaSeq™ 6000 platform.

Raw sequencing reads were processed with FASTP to remove adaptors, low-quality reads, and artifacts, yielding high-quality clean reads. These were aligned to the *Ovis aries* reference genome using HISAT2. Transcript annotation was performed using BLAST, and transcript abundance was normalized to fragments per kilobase of transcript per million mapped reads (FPKM). Differentially expressed genes (DEGs) between groups were identified using a threshold of fold change ≥ 2 and adjusted *P*-value < 0.05 (*padj*), based on multiple testing correction.

2.4. Isolation, culture, and differentiation of sheep myoblasts

Approximately 1 g of fresh *longissimus dorsi* muscle was collected from sheep and rinsed in physiological saline containing 1 % penicillin–streptomycin. The tissue was minced and connective tissue removed, followed by enzymatic digestion with 1 mg/mL type I collagenase for 1 h. The cell suspension was centrifuged at 1000 rpm for 5 min, and the supernatant was discarded. The pellet was resuspended in 0.25 % trypsin solution and digested for 15 min in a water bath. The digestion was stopped by adding an equal volume of growth medium, followed by centrifugation at 1000 rpm for 5 min. After discarding the supernatant, the pellet was resuspended in a small volume of growth medium and passed through a cell strainer to isolate primary myoblasts.

Cells were seeded into culture flasks containing growth medium (DMEM/F12 supplemented with 10 % fetal bovine serum and antibiotics (penicillin and streptomycin) and incubated at 37 °C with 5 % CO₂. The growth medium was replaced every 48 h. When myoblasts reached approximately 90 % confluence, differentiation was induced using a differentiation medium consisting of DMEM/F12 supplemented with 2 % horse serum. Myogenic differentiation were assessed by calculating the fusion index (percentage of nuclei within myosin-positive multinucleated myotubes) [36].

2.5. Cell transfection

Sheep myoblasts were seeded into 12-well plates at a density of 1×10^5 cells per well and cultured until approximately 80 % confluence. Cells were then induced to differentiate by switching to differentiation medium (DMEM supplemented with 2 % horse serum). On day 3 of differentiation, cells were transfected with 100 pmol of si-MAFA or si-NC, or 1.5 µg of pcDNA3.1-MAFA (oe-MAFA) or empty vector pcDNA3.1 (oe-NC) using Lipofectamine 3000 (Invitrogen, Carlsbad, CA, USA), following the manufacturer's protocol. After 48 h of transfection, cells were collected for subsequent assays.

2.6. EDU cell proliferation assay

Sheep myoblasts were enzymatically digested, counted, and adjusted to a concentration of 5×10^4 cells per well. Cells were seeded onto glass coverslips pre-placed in 24-well plates, with 500 µL of cell suspension per well. After 24 h of incubation, cells were transfected using Lipofectamine 3000 (L3000015, Thermo Fisher Scientific, USA) according to the manufacturer's protocol. Briefly, for each well, 75 pmol of siRNA was diluted in 20 µL Opti-MEM medium and mixed with 2.25 µL of Lipofectamine 3000 diluted in another 20 µL of Opti-MEM. The siRNA-lipid complex was incubated at room temperature for 10–15 min and then added to cells in antibiotic-free complete medium. After 48 h, cells were incubated with 50 µM EdU for 2 h using the EDU Cell Proliferation Kit (C0071S, Beyotime, China) according to the manufacturer's instructions. The proportion of proliferating cells was determined by quantifying EDU-positive cells under a fluorescence microscope (CK40, Olympus, Japan).

2.7. Western blotting

Immunoprecipitated (IP) protein samples were subjected to

electrophoresis at 100 V for 1–2 h, followed by overnight protein transfer at 12 V onto a nitrocellulose (NC) membrane. Membranes were blocked at room temperature for 1 h in 5 % blocking solution and incubated overnight at 4 °C with primary antibodies diluted in TBST containing 5 % bovine serum albumin (BSA). After incubation, membranes were washed three times with TBST (5 min each wash), then incubated with HRP-conjugated secondary antibodies diluted in TBST for 1 h at room temperature. After three additional TBST washes, signals were developed using enhanced chemiluminescence (ECL) reagents. Band intensities were quantified using ImageJ software (NIH). The primary antibodies used for Western blot and immunofluorescence are listed in Supplementary Table S1.

2.8. Quantitative real-time PCR (qRT-PCR)

Total RNA was extracted from sheep tissue samples using the TRIzol reagent, and 1 µg of total RNA was reverse transcribed into cDNA using the BeyoRT™ II First Strand cDNA Synthesis Kit (D7168M, Beyotime, China). Quantitative real-time PCR was performed using SYBR Premix Ex Taq™ II on a CFX-96 Real-Time PCR Detection System (Bio-Rad, USA). Experiments were conducted with three biological replicates (independent muscle samples from three lambs) and each qPCR reaction included three technical replicates. Relative gene expression levels were calculated using the 2^{-ΔΔCt} method, with β-actin used as the internal control. The amplification conditions were as follows: an initial denaturation at 95 °C for 10 min, followed by 40 cycles of denaturation at 95 °C for 15 s, annealing at 60 °C for 30 s, and extension at 72 °C for 30 s. Primer sequences used for qRT-PCR are provided in Supplementary Table S2.

2.9. Immunofluorescence

Cultured cells were fixed in 4 % paraformaldehyde and permeabilized with 0.2 % Triton X-100 for 10 min. After blocking with 5 % bovine serum albumin (BSA) in PBS for 1.5 h at room temperature, cells were incubated with primary antibodies overnight at 4 °C. Samples were then washed three times with PBS and incubated with fluorescently labeled secondary antibodies at room temperature. Following another series of PBS washes, nuclei were counterstained with DAPI (C1341S, Beyotime, China) for 10 min. Fluorescent signals were visualized using a fluorescence microscope (CK40, Olympus, Japan).

2.10. Intracellular calcium concentration measurement

Intracellular calcium levels were measured using the Fluo-4 Calcium Assay Kit (S1061S, Beyotime, China). Briefly, cells were seeded into 12-well plates and centrifuged at 250–1000 × g for 5 min. After removing the supernatant, the cells were washed once with PBS. Then, 500 µL of Fluo-4 staining solution was added to each well, and the plates were incubated for 30 min at 37 °C in the dark. Following incubation, the fluorescence staining of the cells was observed under a fluorescence microscope (CK40, Olympus, Japan) with an excitation wavelength of 490 nm and an emission wavelength of 525 nm.

2.11. Statistical analysis

All experiments were performed with at least three biological replicates. The normality of data distributions was assessed using the Kolmogorov–Smirnov test at a significance level of 0.05. Data are presented as the mean ± standard error of the mean (SEM). Differences between two groups were evaluated using Student's *t*-test, while comparisons among more than two groups were performed using one-way analysis of variance (ANOVA) followed by Tukey's multiple comparison test. To assess the relationship between MAFA gene expression and phenotypic traits such as skeletal muscle mass, a linear regression model was used as follows: $Y_i = \beta_0 + \beta_1 X_i + \varepsilon_i$, where Y_i represents the phenotypic trait (e.

g., muscle weight), X_i denotes the relative expression level of MAFA, β_0 is the intercept, β_1 is the regression coefficient, and ε_i is the residual error term. All statistical analyses were performed using SPSS software (version 27.0; SPSS Inc., Chicago, IL, USA). A P -value <0.05 was considered statistically significant. Graphs were generated using GraphPad Prism version 9.5.

3. Results

3.1. MAFA is highly expressed in skeletal muscle tissue

To investigate the tissue-specific expression of MAFA, transcriptomic data from the GTEx project were analyzed across six human tissues as provided by The Human Protein Atlas (<https://www.proteinatlas.org/ENSG00000182759-MAFA/tissue>). Gene expression levels were normalized and represented as nTPM (Transcripts Per Million). Among the examined tissues—skeletal muscle ($n = 803$), testis ($n = 361$), pancreas ($n = 328$), heart muscle ($n = 432$), ovary ($n = 180$), and subcutaneous adipose tissue ($n = 663$)—MAFA showed the highest expression in skeletal muscle, followed by the testis and pancreas (Fig. 1). Notably, MAFA expression in skeletal muscle was significantly higher than in other tissues ($P < 0.001$).

To validate this expression pattern in sheep, we randomly selected three animals from the cohort described in section 2.1 and quantified MAFA transcript levels in six tissues—including the longissimus dorsi muscle—using quantitative real-time PCR (qRT-PCR, $n = 3$). Consistent with the human data, MAFA expression was highest in the longissimus dorsi muscle, with a relative expression level 7.15-fold higher than that in the pancreas (11.776 vs. 1.647).

To explore the potential association between MAFA expression and muscle production performance in sheep, we performed RNA-seq analysis on the *longissimus dorsi* muscle of 30 six-month-old lambs. After slaughter, the left *longissimus dorsi* was weighed. To account for body weight differences, the percentage of *longissimus dorsi* weight relative to carcass weight was used as an indicator of muscle yield. Correlation analysis between this trait and gene expression (normalized as FPKM) revealed a significant positive correlation between MAFA expression and muscle proportion ($P = 0.002$, $R^2 = 0.2837$).

3.2. MAFA shows extensive regulatory activity in skeletal muscle

To investigate tissue-specific roles of MAFA, we performed ChIP-seq and RNA-seq analyses on *longissimus dorsi* muscle and pancreas ($n = 3$ per tissue). ChIP-seq yielded 183.26 M and 204.51 M raw reads for IP and input controls in muscle, and 186.34 M and 183.57 M reads in pancreas (Supplementary Table S3, SRA accession number PRJNA1135757). Clean reads were mapped using Bowtie2, and peaks were called using a q -value <0.05 . A total of 1049 and 471 MAFA binding peaks were identified in muscle and pancreas, respectively. Visualization using IGV confirmed distinct peak distributions between tissues (Fig. 2A). De novo motif analysis (HOMER v4.11.1) identified 41 novel MAFA-binding motifs in sheep (Supplementary Fig. S1), the most significant being GTCAGCAGAC ($P = 1e^{-116}$), which closely matched a known motif from murine pancreatic MAFA ChIP-seq (GSE30298, Score = 0.86) with subtle base preferences (Fig. 2C, Supplementary Table S4).

Differential binding analysis ($|fold change| > 1.2$, $P < 0.05$) identified 1379 peaks associated with 744 genes (Fig. 2E), predominantly located in promoter and intronic regions (Fig. 2F). Transcriptome

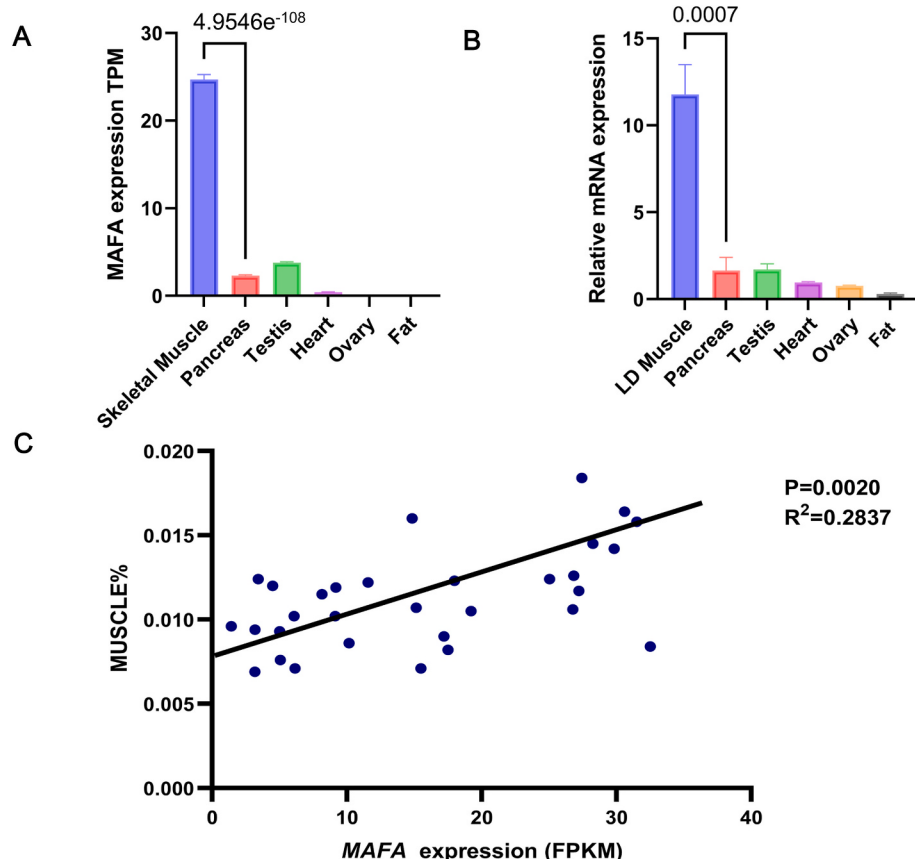


Fig. 1. MAFA is highly expressed in muscle tissue. (A) Expression levels of the MAFA gene (nTPM) in six human tissues from the Human Protein Atlas: skeletal muscle ($n = 803$), testis ($n = 361$), pancreas ($n = 328$), heart muscle ($n = 432$), ovary ($n = 180$), and subcutaneous fat ($n = 663$). Data are presented as mean \pm SEM. (B) Relative expression levels of the MAFA gene in various ovine tissues ($n = 6$). Data are presented as mean \pm SEM. (C) MAFA gene expression (FPKM) in the *longissimus dorsi* muscle is significantly correlated with muscle proportion in sheep ($n = 30$).

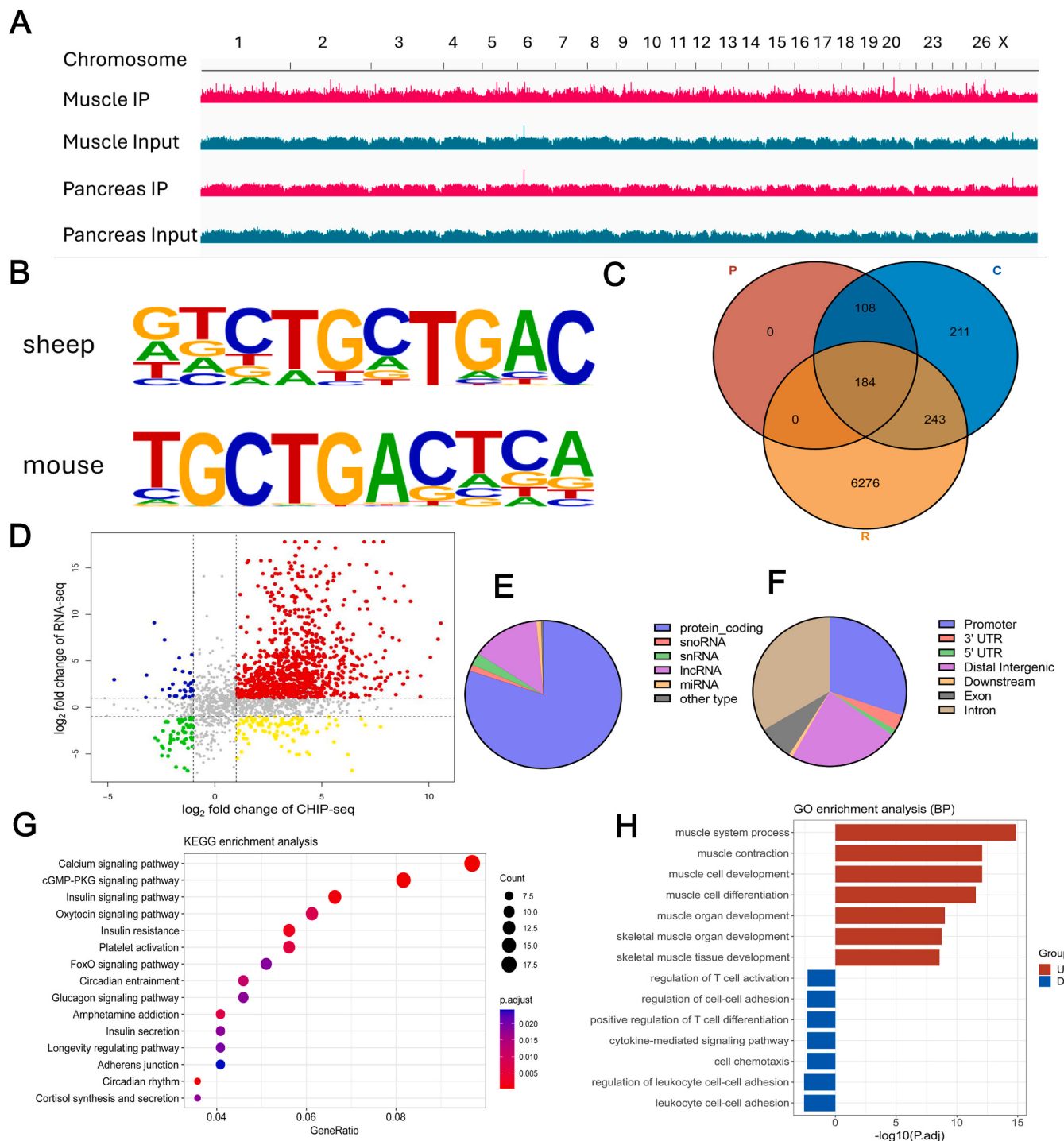


Fig. 2. Integrated analysis of ChIP-Seq and RNA-Seq data. (A) Genomic distribution of MAFA binding peaks in muscle and pancreatic tissues. (B) Comparison of MAFA binding motifs between sheep and mouse (GSE30298) reveals species-specific differences. (C) Identification of MAFA target genes by integrating ChIP-Seq and transcriptomic data. In the Venn diagram, P represents genes with MAFA binding in promoter regions identified by ChIP-Seq; C represents genes with significantly different MAFA binding peaks between muscle and pancreas; R represents differentially expressed genes between muscle and pancreas identified by RNA-Seq. (D) Quadrant plot of genes identified by combined ChIP-Seq and RNA-Seq analyses. (E) Functional annotation of genes with differential MAFA binding peaks between muscle and pancreas. (F) Functional element annotation of MAFA differential binding peaks. (G) KEGG pathway enrichment of MAFA target genes. (H) Bidirectional GO enrichment analysis (Biological Process) of MAFA target genes. ($n = 3$ per tissue).

analysis identified 6703 differentially expressed genes between muscle and pancreas, highlighting distinct transcriptional landscapes. Integration of ChIP-seq and RNA-seq datasets revealed 427 direct MAFA target genes, including 184 with promoter binding (Fig. 2C, D). KEGG enrichment (P -adjusted <0.05) showed significant involvement in 23 pathways, notably cGMP-PKG, calcium signaling, insulin signaling,

insulin resistance, insulin secretion, glucagon signaling, FoxO, and AMPK pathways (Fig. 2G, Supplementary Table S5).

Gene Ontology analysis of biological processes revealed significant enrichment for skeletal muscle development pathways, which were upregulated in *longissimus dorsi* muscle (P -adjusted <0.05 ; Fig. 2H), supporting a role for MAFA in promoting muscle growth in sheep.

3.3. Transcriptional levels of MAFA target genes are associated with muscle yield in sheep

To explore the transcriptional network governed by MAFA and its potential role in muscle development, we performed correlation analyses between gene expression profiles (RNA-seq, $n = 30$, SRA accession number PRJNA1135757) and the percentage of *longissimus dorsi* weight relative to carcass weight. A total of 1778 genes, including MAFA, showed significant correlations with muscle proportion ($P < 0.05$). Comparing these with the 427 direct MAFA target genes identified via ChIP-seq, we found an overlap of 100 genes (Fig. 3A). KEGG pathway enrichment of these overlapping genes (P-adjusted <0.05) revealed three significantly enriched pathways: the FoxO signaling pathway, insulin signaling pathway, and longevity regulating pathway (Fig. 3B; Supplementary Table S6). Ten genes—including *FBXO32*, *SETD7*, *PIK3R1*, *INSR*, *FOXO3*, *EGFR*, *PPARGC1A*, *SORBS1*, *PRKAR2A*, and *RPS6KA3*—were enriched in these pathways, with *PIK3R1* and *INSR* shared across all three. Notably, both genes were also enriched in the insulin resistance pathway (P-adjusted = 0.0516).

Protein–protein interaction (PPI) analysis of the 100 shared genes using STRING v12.0 revealed two distinct sub-networks (Fig. 3C–D). KEGG analysis of sub-network 1 identified calcium signaling as the most significantly enriched pathway (Fig. 3F). This network included *RYR1*, *STIM1*, *CAMK2D*, and *PPP3CA*, all key regulators of calcium homeostasis and signal transduction in muscle, as well as *JPH1*, which is involved in excitation-contraction coupling. Together, 6 out of 12 genes in sub-network 1 were linked to calcium signaling, and all exhibited positive correlations with both muscle proportion and MAFA expression (Fig. 3E).

Sub-network 2 was significantly enriched for the FoxO signaling pathway, insulin signaling pathway, and longevity regulating pathway (Fig. 3H). Among its nine members were *GHR*, *INSR*, and *EGFR*—three membrane-bound receptors involved in growth factor signaling. Expression levels of all genes in this sub-network were positively correlated with both MAFA expression and muscle proportion (Fig. 3G), highlighting their potential roles in MAFA-mediated muscle development.

3.4. MAFA promotes myoblast proliferation and suppresses differentiation

To elucidate the functional role of MAFA in muscle cells, we performed loss- and gain-of-function assays in myoblasts using RNA interference and stable overexpression. Quantitative PCR (Fig. 4A) and Western blotting (Fig. 4B, C) confirmed effective modulation of MAFA expression.

EDU incorporation assays revealed that MAFA overexpression significantly increased the proportion of EDU-positive cells, whereas MAFA knockdown led to a marked decrease in proliferating cells (Fig. 4E, F), indicating that MAFA enhances myoblast proliferation. Consistent with these findings, flow cytometry analysis showed a significant increase in G1-phase cells and a reduction in S-phase cells in the knockdown group, suggesting cell cycle arrest. In contrast, MAFA overexpression reduced the proportion of G1-phase cells and elevated the S-phase population, further supporting a role for MAFA in promoting cell cycle progression and proliferation (Fig. 4G).

We next investigated whether MAFA affects myogenic differentiation. Knockdown of MAFA significantly upregulated MyoG protein levels and increased the myoblast fusion index compared to controls. Conversely, MAFA overexpression resulted in reduced MyoG expression and impaired myotube formation (Fig. 4H, I).

Together, these results demonstrate that MAFA promotes myoblast proliferation while suppressing myogenic differentiation and fusion, indicating a dual role in regulating muscle cell fate.

3.5. MAFA modulates intracellular calcium influx by regulating calcium signaling genes

Given the significant enrichment of MAFA target genes in the calcium signaling pathway identified by ChIP-seq, we hypothesized that MAFA may influence calcium homeostasis in myoblasts through transcriptional regulation of calcium-related genes. To test this, we examined the expression of *STIM1* and *PPP3CA*, two key genes from sub-network 1, in MAFA knockdown and overexpression conditions.

Quantitative PCR analysis showed that MAFA knockdown significantly reduced *STIM1* and *PPP3CA* mRNA levels, while MAFA overexpression resulted in their upregulation (Fig. 5A, B). Western blotting confirmed that STIM1 protein levels were concordant with transcript levels—significantly decreased in the knockdown group and increased in the overexpression group compared to controls (Fig. 5C, D, F, G). However, *PPP3CA* exhibited a different pattern at the protein level: although MAFA overexpression elevated *PPP3CA* protein expression (Fig. 5F, H), MAFA knockdown did not significantly affect its protein level (Fig. 5C, E), suggesting additional post-transcriptional or compensatory regulatory mechanisms modulating *PPP3CA* expression.

To directly assess intracellular calcium levels, we performed calcium imaging using fluorescent calcium indicators. Myoblasts overexpressing MAFA exhibited significantly higher intracellular calcium concentrations than controls, whereas MAFA knockdown led to a marked decrease in calcium influx (Fig. 5I).

These findings demonstrate that MAFA promotes calcium influx in myoblasts by transcriptionally regulating key components of the calcium signaling pathway, thereby contributing to calcium-dependent processes essential for muscle cell growth.

3.6. MAFA activates the PI3K–AKT pathway via receptor tyrosine kinases and induces FOXO3 nuclear exclusion

In pancreatic β cells, MAFA is known to initiate insulin gene transcription. In our study, ChIP-seq analysis revealed that MAFA not only targets *PIK3R1*, but also directly binds to two receptor tyrosine kinase (RTK) genes, *INSR* and *EGFR*. Both encode membrane-bound RTKs that activate the PI3K–AKT signaling cascade, suggesting a broader role for MAFA in modulating insulin responsiveness and cellular metabolism beyond the pancreas.

To validate this regulatory axis, we examined the expression of *PIK3R1*, *INSR*, and *EGFR* in myoblasts subjected to MAFA overexpression or knockdown. qPCR and western blot analysis consistently demonstrated that MAFA overexpression significantly upregulated the mRNA and protein levels of all three genes, whereas knockdown suppressed their expression (Fig. 6A–C, E–I). Furthermore, we assessed downstream activation of AKT by measuring its phosphorylation status. MAFA overexpression markedly increased the ratio of phosphorylated AKT (p-AKT) to total AKT, while knockdown led to a significant reduction (Fig. 6J), confirming PI3K–AKT pathway activation by MAFA.

Interestingly, although *FOXO3* was identified as a direct target of MAFA by ChIP-seq, neither its mRNA nor total protein levels were significantly altered by MAFA manipulation (Fig. 6D–F, K). However, p-FOXO3 levels and the p-FOXO3/FOXO3 ratio were significantly increased in MAFA-overexpressing myoblasts and decreased upon MAFA knockdown (Fig. 6F, K), indicating post-translational regulation of FOXO3 via AKT-mediated phosphorylation.

We further confirmed these results using immunofluorescence. In MAFA-overexpressing cells, FOXO3 phosphorylation was strongly enhanced, with predominant cytoplasmic localization indicative of nuclear exclusion. In contrast, FOXO3 in MAFA knockdown cells was primarily localized in the nucleus (Fig. 6L, M). These results suggest that MAFA indirectly represses FOXO3 transcriptional activity by promoting its phosphorylation through the PI3K–AKT pathway, resulting in its cytoplasmic sequestration. This mechanism prevents FOXO3 from activating catabolic gene programs associated with muscle atrophy.

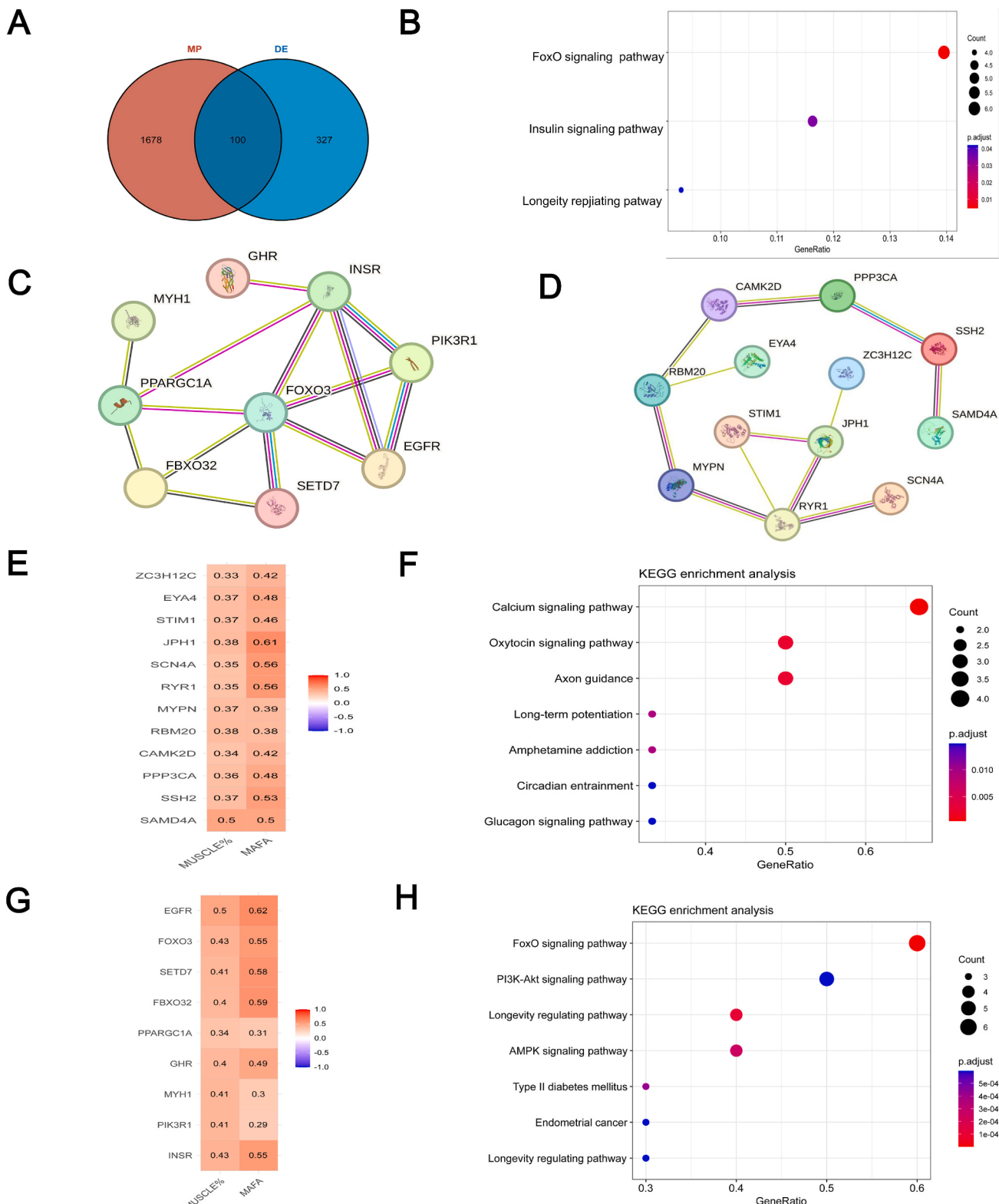


Fig. 3. Transcriptional levels of MAFA target genes are associated with muscle yield in sheep. (A) Venn diagram showing the overlap of genes significantly correlated with longissimus dorsi proportion ($n = 30$) and direct MAFA target genes identified by ChIP-seq. (B) KEGG enrichment analysis of the 100 overlapping genes. (C) Sub-network 1 of protein-protein interaction (PPI) network analysis. (D) Sub-network 2 of PPI network analysis. (E) Heatmap showing that expression of calcium signaling-related genes in sub-network 1 was positively correlated with both MAFA expression and muscle proportion. (F) KEGG enrichment of sub-network 1 genes highlighted calcium signaling as the top pathway. (G) Heatmap showing expression of sub-network 2 genes are positively correlated with MAFA expression and muscle proportion. (H) KEGG enrichment of sub-network 2 revealed significant involvement in FoxO signaling, insulin signaling, and longevity regulating pathways.

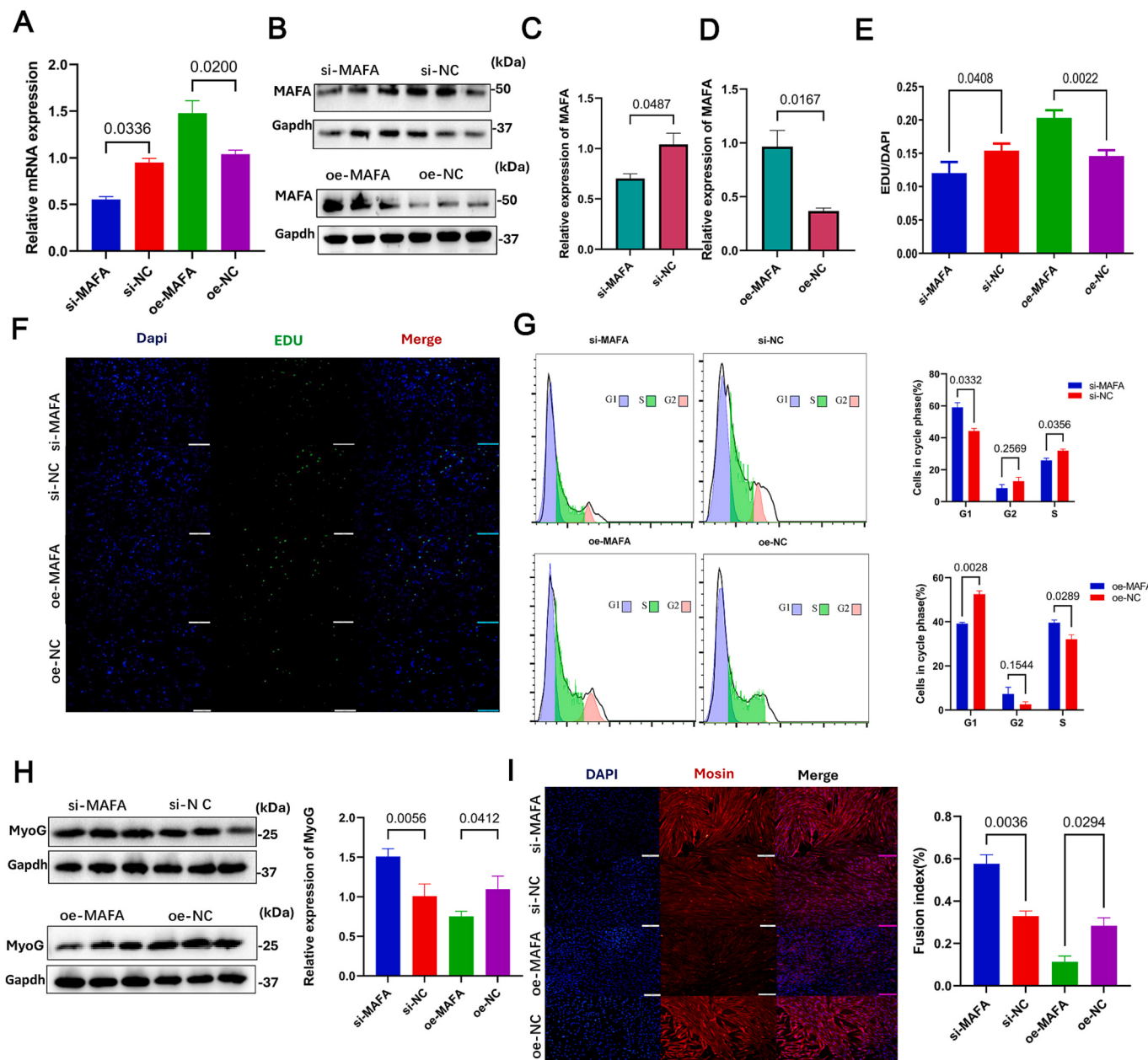


Fig. 4. MAFA promotes myoblast proliferation and inhibits myogenic differentiation. (A) qPCR analysis of MAFA gene expression. (B) Western blot analysis of MAFA protein expression. (C-D) Quantification of MAFA protein levels. (E-F) EdU staining to assess cell proliferation. (G) Cell cycle analysis by flow cytometry. (H) Western blot analysis of the differentiation marker MyoD. (I) Immunofluorescence staining to evaluate myogenic differentiation. $n = 3$. Data are presented as mean \pm SEM.

Collectively, our findings uncover a novel role of MAFA in promoting muscle growth and metabolism by orchestrating the expression of RTKs and downstream PI3K-AKT signaling, culminating in nuclear exclusion of FOXO3.

4. Discussion

MAFA is classically recognized as a β -cell-specific transcription factor that promotes insulin gene transcription. Historically, studies on MAFA have been largely limited to its role in insulin synthesis and pancreatic islet function. However, as MAFA is also expressed in other tissues, recent evidence has proposed broader functional roles for this factor, including potential involvement in neurodegenerative disease, lipid metabolism, tumorigenesis, and muscle fiber development [37]. Nonetheless, these findings remain preliminary, and comprehensive

mechanistic studies are still lacking. In this study, we observed that MAFA is more highly expressed in skeletal muscle than in other tissues, and its expression is positively correlated with the proportion of *longissimus dorsi* muscle, suggesting a previously unreported role in promoting skeletal muscle mass. This has important implications for understanding insulin resistance and muscle atrophy associated with aging and diabetes.

To systematically investigate the role of MAFA in muscle growth, we first sought to identify its direct targets in muscle tissue. Integrated analysis of ChIP-Seq and transcriptomic data revealed that MAFA-binding peaks in *longissimus dorsi* muscle differ substantially from those in the pancreas. These differentially bound genes were significantly enriched in the calcium signaling pathway, cGMP-PKG signaling pathway, and insulin signaling pathway, and include *INSR*, *EGFR*, *PIK3R1*, *CACN1*, *STIM1*, and *MYH1*. To refine the list of functionally

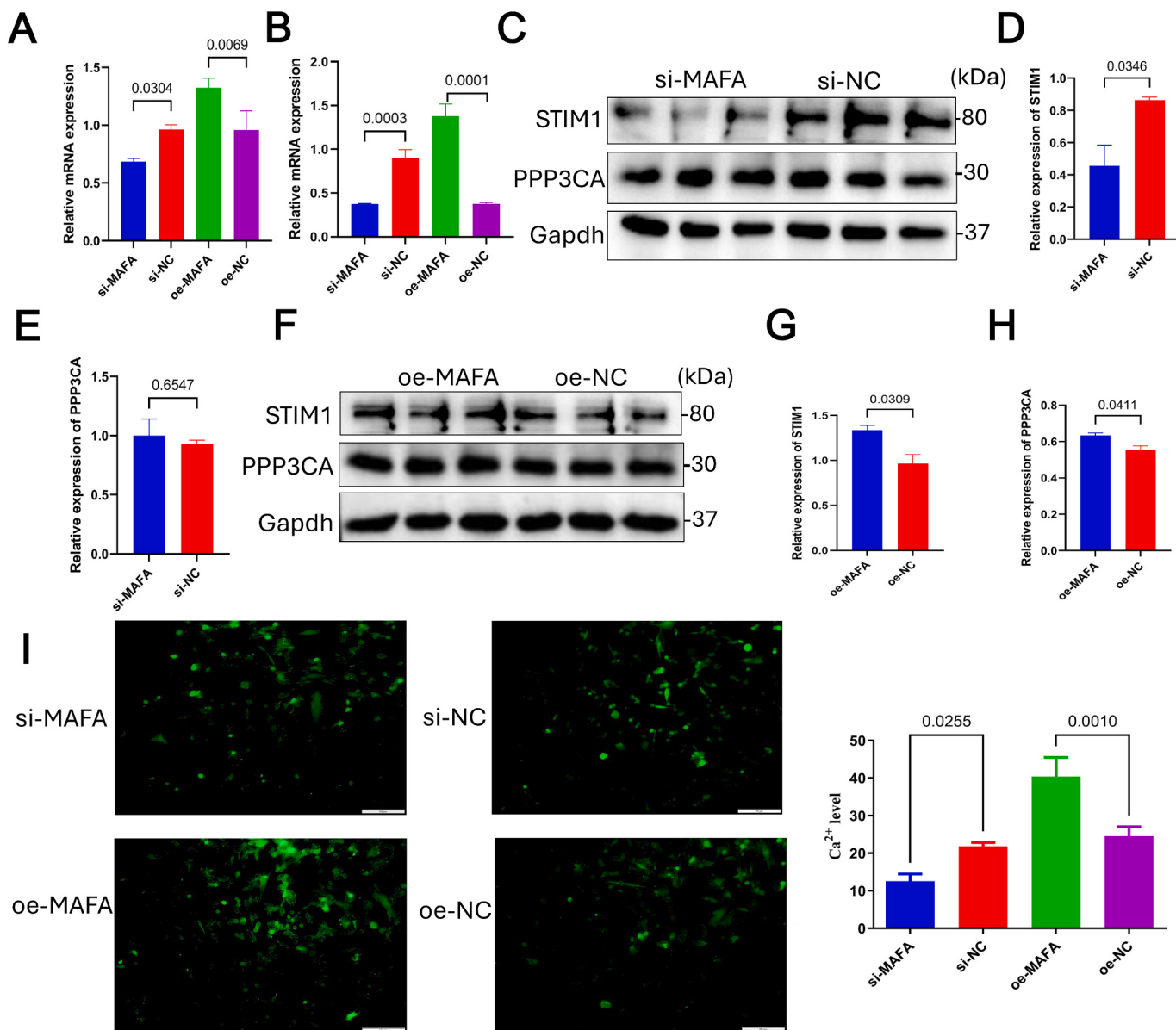


Fig. 5. MAFA mediates intracellular calcium influx in myoblasts by regulating calcium channel gene expression. (A) qPCR analysis of STIM1 gene expression. (B) qPCR analysis of PPP3CA gene expression. (C-E) Western blot analysis of STIM1 and PPP3CA protein levels following MAFA knockdown. (F-H) Western blot analysis of STIM1 and PPP3CA protein levels following MAFA overexpression. (I) Intracellular calcium levels measured using the Fluo-4 AM calcium-sensitive fluorescent probe. $n = 3$. Data are presented as mean \pm SEM.

relevant targets, we intersected these ChIP-Seq genes with genes whose expression was significantly correlated with muscle mass in RNA-Seq data from 30 sheep. Shared genes were considered putative functional targets of MAFA, and protein-protein interaction (PPI) analysis revealed two distinct subnetworks. Subnetwork 1 was most significantly enriched in the calcium signaling pathway (adjusted $p = 0.00045$), while subnetwork 2 was enriched in the FoxO signaling and insulin signaling pathways, and included RTKs such as *INSR* and *EGFR*. These RTKs are known to promote skeletal muscle development by activating signaling cascades via IRS recruitment. Specifically, *INSR* mediates insulin binding to enhance glucose uptake and protein synthesis, whereas *EGFR* facilitates myoblast proliferation and differentiation by activating growth signals [38,39].

These findings suggest that MAFA not only promotes insulin gene transcription in pancreatic islets but also regulates the expression of insulin receptors in muscle tissue, potentially enhancing muscle insulin responsiveness. This dual role highlights MAFA's therapeutic potential

in metabolic diseases characterized by insulin resistance. In addition, MAFA may enhance muscle growth via activation of calcium ion channels and RTK signaling. Functional assays confirmed that MAFA overexpression promotes myoblast proliferation and increases intracellular calcium levels by upregulating the expression of *STIM1* and *PPP3CA*. Calcium signaling plays a central role in muscle cell biology, acting as a second messenger in insulin signaling, glucose uptake, contraction, and differentiation [40,41]. Although *CACN1* has previously been implicated in regulating MAFA expression in knockout mice [37], our ChIP-Seq data identified *CACN1* as a MAFA target (Supplementary Table S5). However, since *CACN1* was not among genes associated with muscle mass in our dataset, we focused on validating *STIM1* and *PPP3CA*. MAFA overexpression significantly enhanced the expression of both genes, indicating a reciprocal regulatory relationship between MAFA and calcium signaling.

Beyond calcium signaling, our data suggest that MAFA promotes muscle growth by upregulating RTK expression. RTK signaling regulates

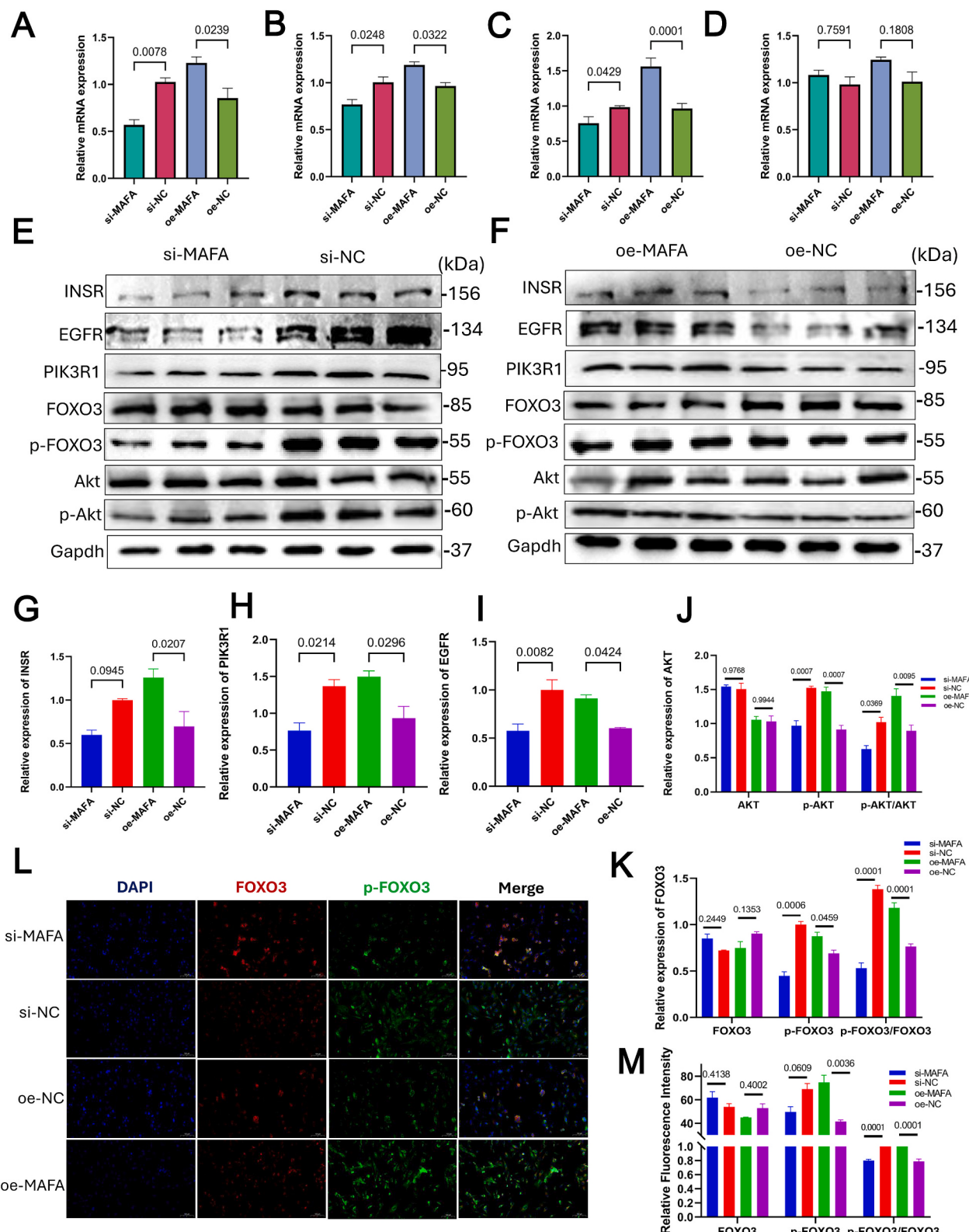


Fig. 6. MAFA activates the PI3K-AKT signaling pathway through receptor tyrosine kinases (RTKs) and induces nuclear exclusion of FOXO3. (A) qPCR analysis of PIK3R1 gene expression. (B) qPCR analysis of INSR gene expression. (C) qPCR analysis of EGFR gene expression. (D) qPCR analysis of FOXO3 gene expression. (E) Western blot analysis of INSR, EGFR, PIK3R1, FOXO3, p-FOXO3, Akt, and p-Akt protein levels following MAFA knockdown. (F) Western blot analysis of the same proteins following MAFA overexpression. (G–I) Quantification of INSR, EGFR, and PIK3R1 protein expression. (J) Relative expression and phosphorylation levels of Akt. (K) Relative expression and phosphorylation levels of FOXO3. (L) Immunofluorescence staining showing the effect of MAFA on FOXO3 phosphorylation and nuclear exclusion. $n = 3$. Data are presented as mean \pm SEM.

downstream pathways including PI3K/Akt and FOXO signaling, which are essential for muscle cell proliferation and survival [42]. MAFA upregulation increased EGFR, INSR, and PIK3R1 expression, resulting in elevated Akt phosphorylation. The PI3K/Akt pathway enhances muscle hypertrophy by promoting protein synthesis and inhibiting degradation [43]. Notably, *GHR*, a gene that indirectly activates PI3K/Akt signaling, was also identified as a MAFA target [44], and its role will be examined in future studies.

Interestingly, we also found that *FOXO3*, a downstream effector of PI3K/Akt, is bound by MAFA. While FOXO signaling promotes muscle protein degradation, phosphorylated FOXO3 is excluded from the nucleus, preventing it from activating catabolic genes [45,46]. Although MAFA overexpression did not alter *FOXO3* transcription levels, it significantly increased *FOXO3* phosphorylation, likely via enhanced Akt activity. Immunofluorescence confirmed *FOXO3* cytoplasmic retention in MAFA-overexpressing cells, consistent with nuclear exclusion and reduced catabolic signaling. These results suggest that MAFA regulates muscle cell proliferation and differentiation via a multifaceted network that integrates calcium signaling, RTK pathways, and *FOXO3*-mediated transcriptional repression.

In addition to the two major mechanisms described above, our ChIP-Seq analysis revealed that MAFA also regulates the transcription of the fast-twitch muscle fiber marker gene *MYH1*. This finding is consistent with previous studies by Dos Santos [37] and Sadaki [10], which demonstrated that MAFA binds to the promoter region of *MYH4* in mouse skeletal muscle. However, our data suggest a species-specific regulatory mechanism: in sheep, MAFA preferentially binds to *MYH1* rather than *MYH4*. Notably, in humans, mice, and other mammals, fast-twitch muscle fiber genes such as *MYH4*, *MYH2*, and *MYH1* are tandemly arranged on the same chromosome, and alternative splicing of their transcripts plays a role in determining fiber type composition. This divergence implies that while MAFA may play a conservative role in promoting fast-twitch fiber identity, the specific downstream targets it regulates differ across species (Fig. 7).

Despite the novel insights provided by this study, several limitations remain. MAFA belongs to the large Maf transcription factor family, which includes members such as *MAFB* and *MAFF* that share similar binding motifs and may exhibit overlapping functions. Our study did not

assess the potential compensatory or cooperative roles of these paralogs in muscle development. In addition, due to the limited number of biological replicates in the ChIP-Seq analysis (three individuals per tissue), some tissue-specific binding events might not have been fully captured. Additionally, while we identified INSR and EGFR as transcriptional targets of MAFA, and both knockdown and overexpression experiments confirmed that MAFA promotes the transcription of these genes, the MAFA binding peaks were more prominent in intronic regions than in canonical promoter regions. This suggests that MAFA may regulate these genes through non-classical regulatory elements, and the precise mechanisms underlying such regulation warrant further investigation.

Moreover, although we confirmed that *MYH1* is a direct target of MAFA in sheep muscle, the binding motif identified differs from the classical MAFA motif. We did not conduct in-depth functional assays to examine how MAFA influences muscle fiber-type specification at the transcriptional level. Further studies are required to validate these findings and clarify whether MAFA serves as a master regulator of fiber-type switching in sheep.

Importantly, all mechanistic experiments were performed *in vitro* using cultured myoblasts, which may not fully recapitulate the *in vivo* muscle environment. Therefore, *in vivo* validation of MAFA's functions is necessary to strengthen the physiological relevance of our conclusions. Furthermore, potential off-target effects of siRNA knockdown were not thoroughly investigated, which could influence the interpretation of functional assays. Future studies should consider more specific gene editing techniques and include *in vivo* models to address these limitations.

5. Conclusions

This study provides the first systematic evidence that MAFA is involved in promoting skeletal muscle growth and development, potentially through calcium ion channels and RTK-related pathways. Our findings identify MAFA as a novel transcriptional regulator in skeletal muscle, expanding its known role beyond pancreatic β -cells. These results reveal new molecular targets for the treatment of muscle-related metabolic disorders and regenerative therapies. With further mechanistic exploration, MAFA may emerge as a potential therapeutic

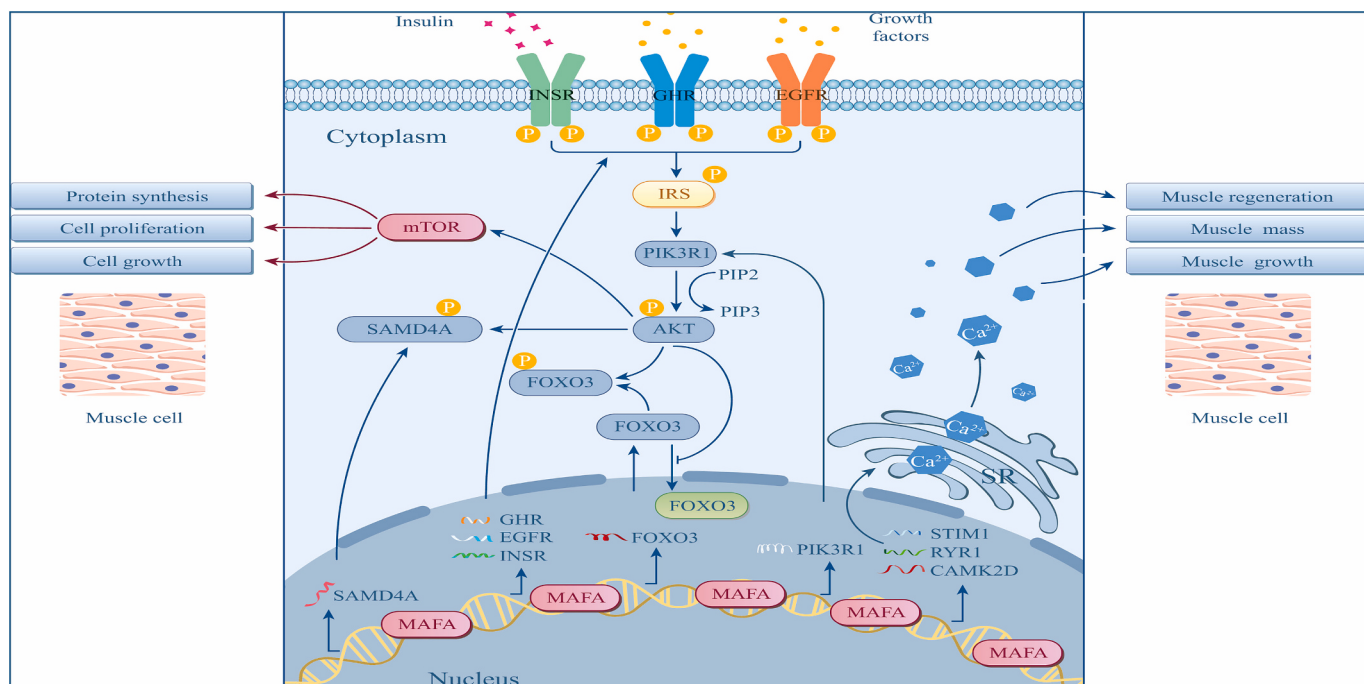


Fig. 7. Schematic diagram of the proposed mechanism by which MAFA regulates muscle growth.

target for insulin resistance, muscular atrophy, and age-related muscle degeneration. Additionally, the regulatory mechanisms uncovered here may offer practical strategies to enhance meat production in livestock, with both scientific and economic significance.

CRediT authorship contribution statement

Cuiyu Lai: Writing – review & editing, Writing – original draft, Methodology. **Yang Chen:** Writing – original draft, Visualization, Methodology. **Xuewen Han:** Methodology. **Yu Fu:** Methodology, Formal analysis. **Jinlin Chen:** Methodology, Formal analysis. **Dandan Tan:** Writing – review & editing. **Xuesong Shan:** Writing – review & editing, Supervision, Conceptualization. **Huaizhi Jiang:** Supervision, Funding acquisition.

Ethics statement

This study and included experimental procedures were approved by the Ethics Committee of Jilin Agricultural University (Approval No. 2022-10-8-012) and were conducted in accordance with the guidelines of the Animal Experimentation Center of Jilin Agricultural University (No. 2021 10 20 001).

Funding

This study was supported by the National Key Research and Development Program of China (2021YFF1000702), the Natural Science Foundation of Jilin Province (20230101254JC), and the Jilin Provincial Key Research and Development Plan Project (20220202038NC).

Declaration of competing interest

The authors declare that they have no known competing financial interests or personal relationships that could have appeared to influence the work reported in the present study.

Appendix A. Supplementary data

Supplementary data to this article can be found online at <https://doi.org/10.1016/j.ijbiomac.2025.146518>.

Data availability

Primer sequences used for RT-qPCR experiments are provided in Supplementary Table S2. The ChIP-seq and RNA-seq data have been submitted to the NCBI Sequence Read Archive (SRA) under BioProject accession number PRJNA1135757 and PRJNA1139683.

References

- [1] M. Nishizawa, K. Kataoka, N. Goto, K.T. Fujiwara, S. Kawai, v-maf, a viral oncogene that encodes a leucine zipper motif, Proc. Natl. Acad. Sci. USA 86 (1989) 7711–7715, <https://doi.org/10.1073/pnas.86.20.7711>.
- [2] K. Kataoka, M. Nishizawa, S. Kawai, Structure-function analysis of the maf oncogene product, a member of the b-Zip protein family, J. Virol. 67 (1993) 2133–2141, <https://doi.org/10.1128/JVI.67.4.2133-2141.1993>.
- [3] K.T. Fujiwara, K. Kataoka, M. Nishizawa, Two new members of the maf oncogene family, mafK and mafF, encode nuclear b-Zip proteins lacking putative trans-activator domain, Oncogene 8 (1993) 2371–2380.
- [4] M. Tsuchiya, R. Misaka, K. Nitta, K. Tsuchiya, Transcriptional factors, Mafs and their biological roles, World J. Diabetes 6 (2015) 175–183, <https://doi.org/10.4239/wjd.v6.i1.175>.
- [5] M. Olbrot, J. Rud, L.G. Moss, A. Sharma, Identification of beta-cell-specific insulin gene transcription factor RIPE3b1 as mammalian MafA, Proc. Natl. Acad. Sci. USA 99 (2002) 6737–6742, <https://doi.org/10.1073/pnas.102168499>.
- [6] W. Nishimura, S. Takahashi, K. Yasuda, MafA is critical for maintenance of the mature beta cell phenotype in mice, Diabetologia 58 (2015) 566–574, <https://doi.org/10.1007/s00125-014-3464-9>.
- [7] L.N. Vanderford, Regulation of β -cell-specific and glucose-dependent MafA expression, Islets 3 (2011) 35–37, <https://doi.org/10.4161/isl.3.1.14032>.
- [8] H. Kaneto, T. Matsuoka, S. Kawashima, K. Yamamoto, K. Kato, T. Miyatsuka, et al., Role of MafA in pancreatic beta-cells, Adv. Drug Deliv. Rev. 61 (2009) 489–496, <https://doi.org/10.1016/j.addr.2008.12.015>.
- [9] T.A. Matsuoka, S. Kawashima, T. Miyatsuka, S. Sasaki, N. Shimo, N. Katakami, et al., MafA enables Pdx1 to effectively convert pancreatic islet progenitors and committed islet α -cells into β -cells in vivo, Diabetes 66 (2017) 1293–1300, <https://doi.org/10.2337/db16-0887>.
- [10] S. Sadaki, R. Fujita, T. Hayashi, A. Nakamura, Y. Okamura, S. Fuseya, et al., Large Maf transcription factor family is a major regulator of fast type IIb myofiber determination, Cell Rep. 42 (2023) 112289, <https://doi.org/10.1016/j.celrep.2023.112289>.
- [11] B.Z. Ring, S.P. Cordes, P.A. Overbeek, G.S. Barsh, Regulation of mouse lens fiber cell development and differentiation by the Maf gene, Development 127 (2000) 307–317, <https://doi.org/10.1242/dev.127.2.307>.
- [12] W. Huang, N. Lu, H. Eberspaecher, B. De Crombrugge, A new long form of c-Maf cooperates with Sox9 to activate the type II collagen gene, J. Biol. Chem. 277 (2002) 50668–50675, <https://doi.org/10.1074/jbc.M206544200>.
- [13] K.E. Merz, D. Thurmond, Role of skeletal muscle in insulin resistance and glucose uptake, Compr. Physiol. 10 (2020) 785–809, <https://doi.org/10.1002/cphy.c190029>.
- [14] J. Argiles, N. Campos, J. López-Pedrosa, R. Rueda, L. Rodríguez-Mañas, Skeletal muscle regulates metabolism via interorgan crosstalk: roles in health and disease, J. Am. Med. Dir. Assoc. 17 (2016) 789–796, <https://doi.org/10.1016/j.jamda.2016.04.019>.
- [15] M. Kanzaki, Insulin receptor signals regulating GLUT4 translocation and actin dynamics, Endocr. J. 53 (2006) 267–293, <https://doi.org/10.1507/endocrj.kr-65>.
- [16] A. Sayem, A. Arya, H. Karimian, N. Krishnasamy, A. Hasamnis, C. Hossain, Action of phytochemicals on insulin signaling pathways accelerating glucose transporter (GLUT4) protein translocation, Molecules 23 (2018) 258, <https://doi.org/10.3390/molecules23020258>.
- [17] M. Li, X. Chi, Y. Wang, S. Setrerrahmane, W. Xie, H. Xu, Trends in insulin resistance: insights into mechanisms and therapeutic strategy, Signal Transduct. Target. Ther. 7 (2022) 216, <https://doi.org/10.1038/s41392-022-01073-0>.
- [18] S.H. Hong, K.M. Choi, Sarcopenic obesity, insulin resistance, and their implications in cardiovascular and metabolic consequences, Int. J. Mol. Sci. 21 (2020) 494, <https://doi.org/10.3390/ijms2120494>.
- [19] A. Ryan, G. Li, S. McMillin, S. Prior, J. Blumenthal, L. Mastella, Pathways in skeletal muscle: protein signaling and insulin sensitivity after exercise training and weight loss interventions in middle-aged and older adults, Cells 10 (2021) 3490, <https://doi.org/10.3390/cells10123490>.
- [20] R.P. Rhoads, L.H. Baumgard, S.W. El-Kadi, L.D. Zhao, PHYSIOLOGY AND ENDOCRINOLOGY SYMPOSIUM: roles for insulin-supported skeletal muscle growth, J. Anim. Sci. 94 (2016) 1791–1802, <https://doi.org/10.2527/jas.2015-0110>.
- [21] F.G. Di Girolamo, C. Biasinutto, A. Mangogna, N. Fiotti, P. Vinci, R. Pisot, et al., Metabolic consequences of anabolic steroids, insulin, and growth hormone abuse in recreational bodybuilders: implications for the World Anti-Doping Agency passport, Sports Med. Open. 10 (2024) 28, <https://doi.org/10.1186/s40798-024-00697-6>.
- [22] E. García-González, C. Brun, M. Rudnicki, J. Hernández-Hernández, The myogenic regulatory factors, determinants of muscle development, cell identity and regeneration, Semin. Cell Dev. Biol. 72 (2017) 10–18, <https://doi.org/10.1016/j.semcdb.2017.11.010>.
- [23] J. Wu, B. Yue, Regulation of myogenic cell proliferation and differentiation during mammalian skeletal myogenesis, Biomed. Pharmacother. 174 (2024) 116563, <https://doi.org/10.1016/j.biophaph.2024.116563>.
- [24] X. Hao, Y. Fu, S. Li, J. Nie, B. Zhang, H. Zhang, Porcine transient receptor potential channel 1 (TRPC1) regulates muscle growth via the Wnt/ β -catenin and Wnt/ Ca^{2+} pathways, Int. J. Biol. Macromol. 265 (2024) 130855, <https://doi.org/10.1016/j.ijbiomac.2024.130855>.
- [25] P.S. Zammit, Function of the myogenic regulatory factors Myf5, MyoD, Myogenin and MRF4 in skeletal muscle, satellite cells and regenerative myogenesis, Semin. Cell Dev. Biol. 72 (2017) 19–32, <https://doi.org/10.1016/j.semcdb.2017.11.011>.
- [26] L. Li, C. Qin, Y. Chen, W. Zhao, Q. Zhu, D. Dai, S. Zhan, J. Guo, T. Zhong, L. Wang, J. Cao, H. Zhang, The novel RNA-RNA activation of H19 on MyoD transcripts promoting myogenic differentiation of goat muscle satellite cells, Int. J. Biol. Macromol. 253 (2023) 127341, <https://doi.org/10.1016/j.ijbiomac.2023.127341>.
- [27] M.A. Roudbar, M.R. Mohammadabadi, A. Ayatollahi Mehrgardi, R. Abdollahi-Arpanahi, M. Momen, G. Morota, F.B. Lopes, D. Gianola, G.J.M. Rosa, Integration of single nucleotide variants and whole-genome DNA methylation profiles for classification of rheumatoid arthritis cases from controls, Heredity 124 (5) (2020) 658–674, <https://doi.org/10.1038/s41437-020-0301-4>.
- [28] S.M.H. Safaei, M. Dadpasand, M. Mohammadabadi, H. Atashi, R. Stavetska, N. Klopenko, O. Kalashnyk, An *Origanum majorana* leaf diet influences myogenin gene expression, performance, and carcass characteristics in lambs, Animals 13 (1) (2023) 14, <https://doi.org/10.3390/ani13010014>.
- [29] M.R. Barazandeh, M. Ghaderi-Zefrehei Mohammadabadi, H. Nezamabadi-Pour, Genome-wide analysis of CpG islands in some livestock genomes and their relationship with genomic features, Czech J. Anim. Sci. 61 (11) (2016) 487–495, <https://doi.org/10.17221/78/2015-CJAS>.
- [30] S. Chen, Y. Zhou, Y. Chen, J. Gu, fastsp: an ultra-fast all-in-one FASTQ preprocessor, Bioinformatics 34 (2018) i884–i890, <https://doi.org/10.1093/bioinformatics/bty560>.
- [31] B. Langmead, S.L. Salzberg, Fast gapped-read alignment with Bowtie 2, Nat. Methods 9 (2012) 357–359, <https://doi.org/10.1038/nmeth.1923>.

- [32] Y. Zhang, T. Liu, C.A. Meyer, J. Eeckhoute, D.S. Johnson, B.E. Bernstein, et al., Model-based analysis of ChIP-Seq (MACS), *Genome Biol.* 9 (2008) R137, <https://doi.org/10.1186/gb-2008-9-9-r137>.
- [33] H. Thorvaldsdóttir, J.T. Robinson, J.P. Mesirov, Integrative genomics viewer (IGV): high-performance genomics data visualization and exploration, *Brief. Bioinform.* 14 (2013) 178–192, <https://doi.org/10.1093/bib/bbs017>.
- [34] G. Yu, L.G. Wang, Q.Y. He, ChIPseeker: an R/Bioconductor package for ChIP peak annotation, comparison, and visualization, *Bioinformatics* 31 (2015) 2382–2383, <https://doi.org/10.1093/bioinformatics/btv145>.
- [35] R. Stark, G. Brown, DiffBind: Differential Binding Analysis of ChIP-Seq Peak Data, R Package Version 100, 2011, p. 4.3. <https://bioconductor.org/packages/release/bioc/html/DiffBind.html>.
- [36] X. Zhang, L. He, L. Wang, Y. Wang, E. Yan, B. Wan, Q. Zeng, P. Zhang, X. Zhao, J. Yin, CLIC5 promotes myoblast differentiation and skeletal muscle regeneration via the BGN-mediated canonical Wnt/β-catenin signaling pathway, *Sci. Adv.* 10 (2024) eadq6795, <https://doi.org/10.1126/sciadv.adq6795>.
- [37] M. Dos Santos, A.M. Shah, Y. Zhang, S. Bezprozvannaya, K. Chen, L. Xu, et al., Opposing gene regulatory programs governing myofiber development and maturation revealed at single nucleus resolution, *Nat. Commun.* 14 (2023) 4333, <https://doi.org/10.1038/s41467-023-40073-8>.
- [38] A. Cignarelli, V.A. Genchi, S. Perrini, A. Nataleicchio, L. Laviola, F. Giorgino, Insulin and insulin receptors in adipose tissue development, *Int. J. Mol. Sci.* 20 (2019) 759, <https://doi.org/10.3390/ijms20030759>.
- [39] A.W. Burgess, Regulation of signaling from the epidermal growth factor family, *J. Phys. Chem. B* 126 (2022) 7475–7485, <https://doi.org/10.1021/acs.jpcb.2c04156>.
- [40] A. Agrawal, G. Suryakumar, R. Rathor, Role of defective Ca^{2+} signaling in skeletal muscle weakness: pharmacological implications, *J. Cell Commun. Signal.* 12 (2018) 645–659, <https://doi.org/10.1007/s12079-018-0477-z>.
- [41] J. Levin, L. Borodinsky, M. Tu, A. Hamilton, Calcium signaling in skeletal muscle development, maintenance and regeneration, *Cell Calcium* 59 (2016) 91–97, <https://doi.org/10.1016/j.ceca.2016.02.005>.
- [42] M. Lawlor, X. Feng, D. Everding, K. Sieger, C. Stewart, P. Rotwein, Dual control of muscle cell survival by distinct growth factor-regulated signaling pathways, *Mol. Cell. Biol.* 20 (2000) 3256–3265, <https://doi.org/10.1128/MCB.20.9.3256-3265.2000>.
- [43] X. Zhou, Y. Ding, C. Yang, C. Li, Z. Su, J. Xu, et al., FHL3 gene regulates bovine skeletal muscle cell growth through the PI3K/Akt/mTOR signaling pathway, *Comp. Biochem. Physiol. D Genomics Proteomics.* 52 (2024) 101356, <https://doi.org/10.1016/j.cbd.2024.101356>.
- [44] J. Yu, W. Cui, Proliferation, survival and metabolism: the role of PI3K/AKT/mTOR signalling in pluripotency and cell fate determination, *Development* 143 (2016) 3050–3060, <https://doi.org/10.1242/dev.137075>.
- [45] K. Chen, P. Gao, Z. Li, J. Su, Z. Deng, Forkhead box O signaling pathway in skeletal muscle atrophy, *Am. J. Pathol.* 192 (2022) 1648–1657, <https://doi.org/10.1016/j.ajpath.2022.09.003>.
- [46] M. Savova, L. Mihaylova, D. Tews, M. Wabitsch, M. Georgiev, Targeting PI3K/AKT signaling pathway in obesity, *Biomed. Pharmacother.* 159 (2023) 114244, <https://doi.org/10.1016/j.biopha.2023.114244>.